Viscosity and Free Energy Dependence of Photochemical Charge Separation

A. I. Burshtein*

Department of Chemical Physics, Weizmann Institute of Science, 76100 Rehovot, Israel

N. V. Shokhirev†

Department of Chemistry, The University of Arizona, Tucson, Arizona 85721

Received: July 23, 1996; In Final Form: October 10, 1996⊗

Contrary to the conventional ("exponential") model of contact charge creation and recombination, we consider here a recombination of a geminate ion pair occurring in a remote rectangular spherical layer. This simple model available for analytical solution enables one to discriminate between inner and outer generation of charges with respect to a thin recombination layer. In the slow diffusion limit, the qualitatively different viscosity and free energy dependencies of effective recombination rate are predicted for these alternative cases. The experimental verification of these predictions can provide clear evidence of noncontact electron transfer in liquid solutions.

1. Introduction

In the "exponential model" of geminate charge recombination[1] the ions are assumed to appear only at contact distance σ and then either recombine at the same distance or separate according to the kinetic scheme

$$[\mathrm{D}\cdots\mathrm{A}] \Leftarrow [\mathrm{D}^+\cdots\mathrm{A}^-] \Rightarrow \mathrm{D}^+ + \mathrm{A}^- \qquad (1.1)$$

In a few recent articles we showed that such a simplified treatment is erroneous when ions are either created far from the contact or recombine far from it.[2−4] The ionization following the light excitation of the donor (D) is a binary reaction with electron acceptors (A)

$$\mathrm{D}^* + \mathrm{A} \Rightarrow [\mathrm{D}^+\cdots\mathrm{A}^-] \qquad (1.2)$$

which is contact only in Marcus' normal region (when ionization free energy $|\Delta G_\mathrm{i}|$ is less than reorganization energy of surrounding λ_c) and under kinetic control. The recombination is also contact only in the normal region, where corresponding free energy $|\Delta G_\mathrm{r}| \ll \lambda_\mathrm{c}$. In inverted Marcus' regions both ionization and recombination occur far from the contact, in remote reaction layers.[5,6]

The problem is that the excitation energy of donor

$$\epsilon_0 = -\Delta G_\mathrm{I} - \Delta G_\mathrm{R} \qquad (1.3)$$

is usually so large that both free energies can hardly be small simultaneously. For instance, if

$$\epsilon_0 = 2\lambda_\mathrm{c} \qquad (1.4)$$

is kept constant, there are only two possibilities shown in Figure 1a: either ionization is normal but recombination is inverted (NI case) or *vice versa* (IN case). In the NI case ions born in contact recombine far from it, while in the IN case they enter the recombination layer from outside where they were initially created.

The latter situation is rather usual and may be analyzed within "contact approximation" assuming the width of adjoined recombination layer $L \to 0$.[7,8] This approximation employed in ref 4 for analysis of charge separation quantum yield in the IN case is inappropriate for the NI case where L is an essential parameter determined from the transparency of the outer recombination layer. Here we use the rectangular approximation of the recombination layer to keep L finite and gain the analytical solution of the problem. Although this approximation was used

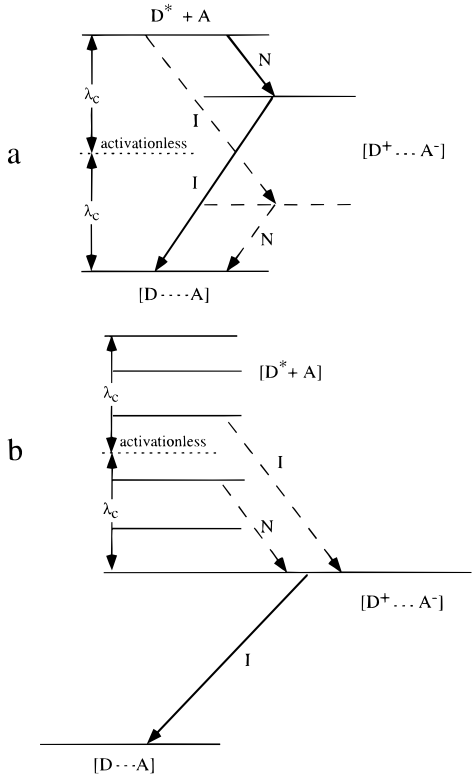

Figure 1. Scheme of energy levels and electron transitions: (a) at fixed excitation energy $\epsilon = 2\lambda_\mathrm{c}$ but different positions of charge transfer state (the forward and backward electron transitions corresponding to the IN case are depicted by dashed arrows, while those related to the NI case are shown by solid arrows; (b) at fixed free energy of recombination $\Delta G_\mathrm{r} = \mathrm{const}$ but arbitrary ionization free energy. The forward electron transitions from excited states of different donors (dashed arrows) are followed by the common backward transition to a ground state (solid arrow).

† On leave from Institute of Chemical Kinetics and Combustion RAS, Novosibirsk, 630090 Russia.

⊗ Abstract published in *Advance ACS Abstracts,* December 1, 1996.

S1089-5639(96)02217-7 CCC: $14.00

a few times for analysis of luminescence quantum yield[9] or kinetics of forward electron transfer (eq 1.2)[10] to back electron transfer (eq 1.1), it has not been applied until recently.[11] However, the authors of ref 11 concentrated mainly on kinetics of geminate recombination in the limit of large L. On the contrary, our consideration is confined to only charge separation quantum yield which will be rigorously obtained for arbitrary L and any initial ion separation r_0.

The separation quantum yield is given by the general formula

$$\varphi = \frac{1}{1 + Z/\tilde{D}} \tag{1.5}$$

where $\tilde{D}$ is a coefficient of encounter diffusion of ions. This is an essential result first obtained within the *exponential model*[1] which operates with a distant independent, single rate constant k_{-et} which is the same for all reactants in a spherical cage of radius σ where ions are initially created. The total number of ions $n = n_c + n_\infty$ is combined from those in the case (n_c) and the rest (n_∞) that jumped out with the rate k_{sep}. The solution of corresponding kinetic equations

$$\dot{n}_c = -k_{-et}n_c - k_{sep}n_c$$

$$\dot{n}_\infty = k_{sep}n_c \tag{1.6}$$

with obvious initial conditions $n_c(0) = 1$, $n_\infty(0) = 0$ leads to an exponential relaxation of $n(t)$ to φ

$$\frac{n - \varphi}{1 - \varphi} = e^{-(k_{-et}+k_{sep})t}$$

Owing to this kinetics, the model is known as *exponential*. Unfortunately, the real relaxation is never exponential (either in polar[8] or in nonpolar solutions[12]) so that only experimental data on the separation quantum yield are worthy of comparison with the exponential model. The main conclusion of the latter is that $Z \equiv z$ is the universal, diffusion independent factor determining quantum yield:

$$\varphi = \frac{1}{1 + k_{-et}/k_{sep}} = \frac{1}{1 + z/\tilde{D}}, \quad \text{where} \quad k_{sep} = \frac{3r_c\tilde{D}}{\sigma^3[e^{r_c/\sigma} - 1]}$$

In the highly polar solvents considered here, the Onsager radius $r_c \ll \sigma$ and $k_{sep} = 3\tilde{D}/\sigma^2$ so that

$$z = k_{-et}\sigma^2/3 = \text{const} \tag{1.7}$$

at any diffusion.

However, Z is not really identical to z. In *contact approximation* the recombination which is still considered as contact is given by kinetic rate constant k_0 simply related to k_{-et}:[8]

$$k_0 = k_{-et}4\pi\sigma^3/3 = 4\pi\sigma z$$

However, the initial separation of ions r_0 may exceed contact distance and is kept free as a fitting parameter. As a result, φ depends on r_0[7,8] as well as Z which is always smaller than z and increases with diffusion approaching the fast diffusion limit from below:[4]

$$Z(\tilde{D}) = \frac{\kappa z}{1 + \dfrac{1 - \kappa}{\tilde{D}}z} \to \kappa z \quad \text{at} \quad \tilde{D} \to \infty \tag{1.8}$$

Here $\kappa = \sigma/r_0 \le 1$. In our nonmodel *unified theory* of photoseparation[3] such a behavior of $Z/\tilde{D}$ was attributed to only the IN case (remote recombination, contact ionization) and therefore has a reasonable explanation within contact approximation.[4] Alternatively, in the NI case, the diffusional behavior of Z was found to be quite the opposite. The nonmodel theory showed that $Z \ge z$ and $\lim_{\tilde{D}\to\infty}Z$ is approached from above.[3] This fact was not given the interpretation although the suggestion was made that it results from inner generation of ions, deep inside the recombination layer. Here we are able to prove this statement (section 2) because the rectangular model is good not only for outer ionization (as contact approximation) but also for inner ionization with respect to recombination layer.

With this model we will also demonstrate that the separation quantum yield does not change until the initial separation of ions is less than the inner radius of recombination layer but sharply increases as soon as the interion distance exceeds the external radius of the reaction layer. This observation has opened up fresh opportunities for discrimination between inner and outer ionization which are complementary to those discussed above. If there is a row of donors different in excitation energy ϵ, then one may increase the ionization energy $|\Delta G_i|$ keeping the recombination free energy the same:

$$\Delta G_r = \text{const} \tag{1.9}$$

As seen from Figure 1b, the situation changes with $|\Delta G_i|$ from normal-inverted (NI) to inverted-inverted case (II). As a result, the ionization layer moves away while position of recombination layer remains fixed due to eq 1.9. Using our nonmodel theory (section 3), we confirmed the expansion of initial ion distribution from inside to outside the recombination layer and qualitative change of $\bar{\varphi}(\Delta G_i)$ behavior at the threshold $|\Delta G_i| = \lambda_c$ which is a border between NI and II cases. At the latter case the separation quantum yield significantly increases with $-\Delta G_I$ instead of being constant as in the exponential model.

2. Rectangular Recombination Layer

If the electron transfer near the contact is inverted being normal far from it, then in between it is activationless and the fastest. Hence, the position dependent rate of back electron transfer $W_R(r)$ has a bell shape with a maximum located near the activationless spherical layer $r = r_a > \sigma$.[5,6,13] The rectangular approximation of this function should be written as follows

$$W_R = \begin{cases} 0 & \sigma < r < r_1 \\ W & r_1 < r < r_2 \\ 0 & r_2 < r < \infty \end{cases} \tag{2.1}$$

where $r_1 < r_a < r_2$. The width of recombination layer $L = r_2 - r_1$, and the rate of recombination W should be adjusted to approximate well the real $W_R(r)$ dependence. The similar approximation for $W_I(r)$ was used a few times within binary encounter theory to calculate the nonstationary ionization either in contact[14] or in remote reaction layer.[15] Now we concentrate on geminate recombination in such a polar solvent that Coulombic attraction in the ion pair is negligible. Then the equation for the separation quantum yield of ions initially divided by distance r_0 takes the following form[16]

$$W_R(r_0)\,\varphi(r_0) = \frac{\tilde{D}}{r_0^2}\frac{\partial}{\partial r_0}r_0^2\frac{\partial}{\partial r_0}\varphi(r_0) \tag{2.2}$$

with boundary conditions

$$\frac{\partial}{\partial r_0}\varphi(r_0)|_\sigma = 0 \qquad \varphi(\infty) = 1 \tag{2.3}$$

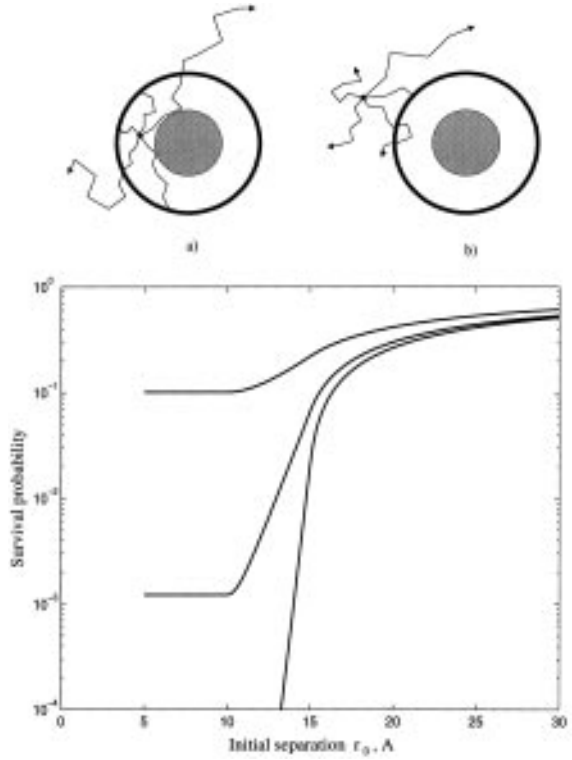

Figure 2. Separation quantum yield (survival probability at $t = \infty$) as a function of initial distance between the ions for $\tilde{D} = 10^{-5}$ cm^2/s and three recombination rates (from top to bottom), $W = 10$, 100,1000 ns^{-1} ($\sigma = 5$ Å, $r_1 = 10$ Å, $L = 5$ Å). Above: (a) start from inside recombination layer related to the left, horizontal branches of the curves and (b) the outside start related to the right branches approaching the maximum $\varphi = 1$.

Using eq 2.1 in eq 2.2 we obtain the following solution

$$\varphi(r_0) = \begin{cases} 2/C & \sigma < r_0 < r_1 \\ [(qr_1 + 1)e^{q(r_0 - r_1)} + & \\ \quad (qr_1 - 1)e^{-q(r_0 - r_1)}]/Cqr_0 & r_1 < r_0 < r_2 \\ 1 - (r_1 + L)/r_0 + [(qr_1 + 1)e^{qL} + & \\ \quad (qr_1 - 1)e^{-qL}]/Cqr_0 & r_2 < r_0 < \infty \end{cases} \quad (2.4)$$

where

$$C = (qr_1 + 1)e^{qL} - (qr_1 - 1)e^{-qL}, \quad q = \sqrt{\frac{W}{\tilde{D}}} \quad (2.5)$$

At $qL \gg 1$ these expressions reduce to those obtained in ref 11.

As is seen, the quantum yield does not depend on initial separation as long as it is less than the inner radius of recombination layer r_1. The recombination layer screens the ions started from inside. The separation quantum yield is the smaller the faster the recombination but sharply increases when the starting point is shifted outside (Figure 2).

The same happens when diffusion becomes slower. With increase of the residence time in the recombination layer, $\tau_e = r_1 L/\tilde{D}$, the layer becomes nontransparent for particles started from inside (Figure 3). The quantum yield of these particles may be represented as

$$\varphi(r_0 < r_1) = \frac{1}{\cosh(qL) + qr_1 \sinh(qL)} \quad (2.6)$$

and its fast diffusion limit

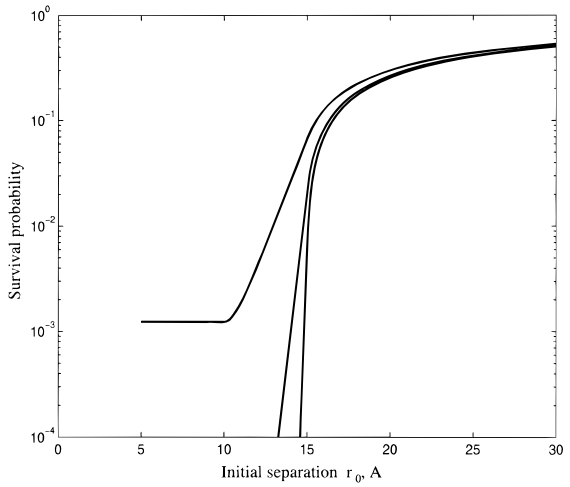

Figure 3. Separation quantum yield (survival probability at $t = \infty$) as a function of initial distance between the ions for $W = 100$ ns^{-1} and three diffusion coefficients (from top to bottom) $\tilde{D} = 10^{-5}$, 10^{-6}, 10^{-7} cm^2/s. The rest of the parameters are the same as in Figure 2.

$$\lim_{q \to 0} \varphi(r_0 < r_1) = \frac{1}{1 + Wr_1 L/\tilde{D}} \quad (2.7)$$

is actually reached at

$$qL = \sqrt{\frac{WL^2}{\tilde{D}}} \ll 1 \quad (2.8)$$

Under this condition the recombination during a single diffusional crossing of the reaction layer ($\tau_c = L^2/\tilde{D}$) is small. However, the total effect, represented by term $W\tau_e = (ql)^2(r_1/L)$ in eq 2.7, may be large if the number of crossings, $\tau_e/\tau_c = r_1/L$, is large.

The limit (eq 2.7) coincides with what was predicted by the exponential model if one sets

$$z = WLr_1 \quad (2.9)$$

that is, $k_{-e} = 3WLr_1/\sigma^2 = k_r/v$ where $k_r = 4\pi r_1^2 LW$ and $v = 4\pi r_1^3/3$.[8] On the other hand, from comparison of eqs 1.8 and 2.6 we obtain

$$Z = z[\cosh(qL) + qr_1 \sinh(qL) - 1]/q^2 Lr_1 \quad (2.10)$$

that deviates significantly from z at slower diffusion (higher viscosity) (Figure 4). The deviation is the smaller the thinner the recombination layer; passing to the limit $L \to 0$ at $z = \text{const}$ one returns back to an exponential model result, eq 2.8.

If ions are created outside the recombination layer, then the separation quantum yield may be written as

$$\varphi(r_0 \geq r_2) = 1 - \frac{r_1 + L}{r_0} + \frac{qr_1 \cosh(qL) + \sinh(qL)}{qr_0 \cosh(qL) + q^2 r_0 r_1 \sinh(qL)} \quad (2.11)$$

If condition 2.8 is met, this result may be simplified to the following

$$\varphi(r_0 \geq r_2) \approx 1 - \frac{r_2}{r_0}\frac{q^2 r_1 L}{1 + q^2 r_1 L} = 1 - \frac{r_2}{r_0}\frac{k_r}{k_r + k_D} \quad (2.12)$$

where k_r and $k_D = 4\pi r_1 \tilde{D}$ are kinetic and diffusional rate constants. An essential parameter $q^2 r_1 L = k_r/k_D \lessgtr 1$ is exactly the same as in contact approximation.[8] By equating expression

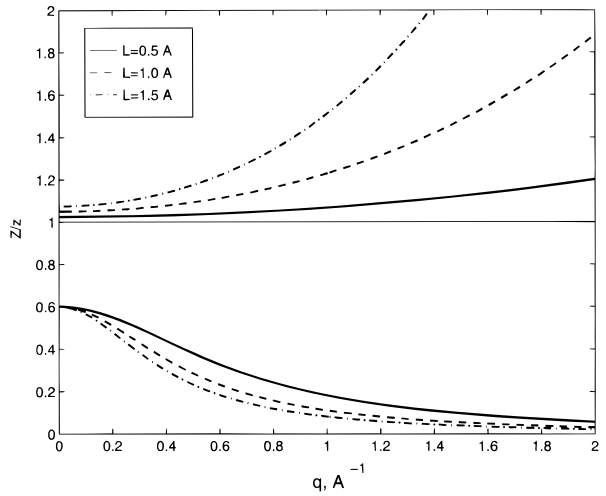

Figure 4. (top) Deviations from the exponential model result ($Z \equiv z$) for ions starting from inside the recombination layer of different widths L. (bottom) the same for outside start, from $r_0 = 20$ Å $> r_2 = 12$ Å.

2.12 to 1.8 we obtain

$$Z = \frac{r_2}{r_0}\frac{z}{1 + \left(1 - \frac{r_2}{r_0}\right)q^2 r_1 L} \tag{2.13}$$

that does not coincide with z and slightly differs from it even in the fast diffusion limit:

$$\lim_{q\to 0} Z = \frac{r_2}{r_0} z < z \tag{2.14}$$

This "quasi-kinetic limit" is actually reached from below (Figure 4) as it was discovered in ref 4. Thus, the diffusional (viscosity) dependence of Z is really the opposite when ions start from inside and outside the recombination layer.

3. Smooth Recombination Layer and Real Initial Distribution

The position dependent rate of ion recombination due to electron transfer is

$$W_R(r) = w_r(r)\, e^{-U_R/T} \quad (k_B = 1) \tag{3.1}$$

If the process is assisted by one solvent mode considered classically, the activation energy

$$U_R(r) = \frac{(\Delta G_r + \lambda)^2}{4\lambda}$$

depends quadratically on the *free energy* of the recombination ΔG_r.[17] The single parameter of this dependence, the *reorganization energy* $\lambda(r)$, is actually a measure of the electron's interaction with the solvent. In highly polar solvents only this parameters of U_R is r-dependent

$$\lambda = \lambda_c + \frac{e^2}{\epsilon_0}\left[\frac{1}{\sigma} - \frac{1}{r}\right]$$

where λ_c is the reorganization energy at contact, e is charge of electron, and ϵ_0 is optical dielectric permitivity of the solvent. For highly exothermic recombination the electron transfer at contact usually occurs in the inverted region ($-\Delta G_r > \lambda_c$) but becomes activationless at larger distance r_a where $-\Delta G_r = \lambda(r_a)$.[6] Being activated (and therefore small) at contact, the rate

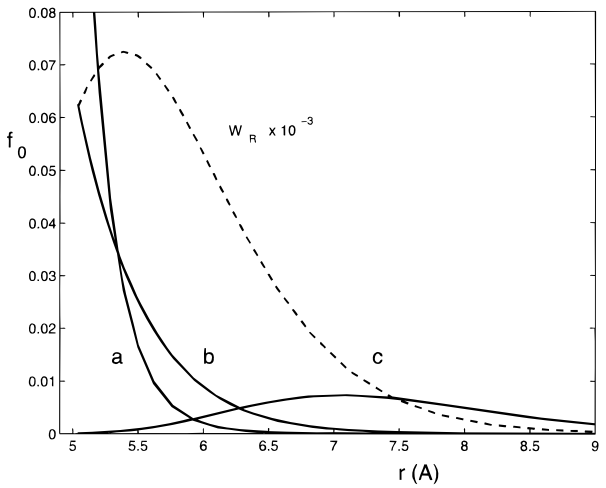

Figure 5. Initial distributions of ions for (a) $|\Delta G_i| = 0$, (b) $|\Delta G_i| = \lambda_c$, (c) $|\Delta G_i| = 2\lambda_c$ in comparison with recombination rate $W_R(r)$ (dashed line). The other parameters are $w_i = 1.3 \times 10^3$ ns^{-1}, $\lambda_c/T = 55$, $T = 300$ K, $|\Delta G_r| = 1.5\ \lambda_c$, $\sigma = 5$ Å.

(eq 3.1) passes through the maximum near r_a and then decreases with further increase of distance (dashed line in Figure 5). The bell-shaped $W_R(r)$ is not rectangular any more and should be compared with initial distribution of ions which is also smooth in reality, not a δ-function at r_0 as in the previous section.

To find initial distribution generated by binary photochemical reaction (eq 1.8), one should use an encounter theory developed in ref 2 and position dependent rate of ionization similar to eq 3.1

$$W_I(r) = w_i(r)\, e^{-U_I/T} \quad (k_B = 1) \tag{3.2}$$

where

$$U_I(r) = \frac{(\Delta G_i + \lambda)^2}{4\lambda}$$

but λ is the same. The normalized initial distribution of ions is

$$f_0(r) = m_0(r)/\int m_0(r)\, d^3r \tag{3.3}$$

where $m_0(r)$ results from ionization and is given by relation 12 from ref 2:

$$m_0 = W_I(r) \int_\sigma^\infty n(r,t)\, N(t) 4\pi r^2\, dr \tag{3.4}$$

The integrand in eq 3.4 should be found by means of conventional encounter theory. The kinetic equation for the excitation density

$$\dot{N} = -k_I(t) c N - N/\tau_D \tag{3.5}$$

should be solved with an initial condition $N(0) = 1$. Here τ_D is the lifetime of the excitation, while $k_I(t)$ is a time-dependent rate constant of ionization defined through the pair distribution function of reactants $n(r,t)$:

$$k_I(t) = \int_\sigma^\infty W_I(r)\, n(r,t) 4\pi r^2\, dr \tag{3.6}$$

To use this definition one has to solve preliminary the auxiliary kinetic equation for n

$$\dot{n} = -W_I(r) n + \frac{D}{r^2}\frac{\partial}{\partial r} r^2 \frac{\partial}{\partial r} n \tag{3.7}$$

where D is a coefficient of encounter diffusion of reactants. Since the position dependent rate in eqs 3.6 and 3.7 accounts for the reaction, wherever it happens the reflecting boundary condition must be used

$$\left.\frac{\partial}{\partial r}\right|_{\sigma} = 0 \tag{3.8}$$

together with the initial condition

$$n(r,0) = 1 \tag{3.9}$$

assuming that the reactants were uniformly distributed at the beginning. Using a program developed in ref 4, we solved numerically these equations and used n and N in eq 3.4 to find thereafter from eq 3.3 the normalized initial distributions $f_0(r)$ at any given ionization free energy ΔG_i. Some of them are shown by solid lines in Figure 5. The larger is $|\Delta G_i|$ the wider becomes the distribution that finally acquires the bell shape with a maximum shifted out of the recombination layer. The average distance between the ions increases accordingly being initially less and finally larger than the external recombination radius.

Therefore one should expect that the charge separation quantum yield should increase with $|\Delta G_i|$ as was the case previously with r_0. If there were a family of donors having different energies of excited state D^* but the same energy of electron transfer state in a pair $D^+\cdots A^-$ (Figure 1b), then it might be proved experimentally that the ionization free energy significantly affects the separation quantum yield. The exponential model does not provide this effect in principle because all initial distances except contact are excluded from the beginning.

In general the photoseparation quantum yield

$$\phi = \psi\bar{\varphi} \tag{3.10}$$

is a product of the photoionization quantum yield

$$\psi = c\int_{\sigma}^{\infty} m_0(r) 4\pi r^2 \, dr \tag{3.11}$$

and the charge separation quantum yield

$$\bar{\varphi} = \int_{\sigma}^{\infty} \varphi(r) \, f_0(r) 4\pi r^2 \, dr \tag{3.12}$$

averaged over initial distribution of ions $f_0(r)$. The factor ψ may be ignored when one deals with a long-lived excited donor because

$$\psi = 1 \quad \text{at} \quad \tau_D = \infty \tag{3.13}$$

In this particular case

$$\phi \equiv \bar{\varphi} = \frac{1}{1 + Z/\tilde{D}} \tag{3.14}$$

One may calculate φ solving eq 2.2 with $W_R(r)$ from eq 3.1 as it was done in ref 18. Then the solution obtained should be averaged with $f_0(r)$ as indicated in eq 3.12. In fact, the results shown in Figure 6 were calculated more generally, using a program developed by Dr. Krissinel[3] that generates simultaneously initial distributions, recombination kinetics, and separation quantum yield with a proper account for Coulombic attraction if necessary. We addressed the case of water where Onsager's radius is rather small (7 Å) and does not play a significant role. As expected, the averaged separation quantum yield begins to sharply increase as soon as $|\Delta G_i|$ becomes larger than $|\Delta G_r|$. Under this condition the ionization radius exceeds the recombination one and ions are generated outside the reaction layer. The experimental confirmation of this dependence would be the best qualitative evidence in favor of present theory and against the primitive exponential model which is still in use.

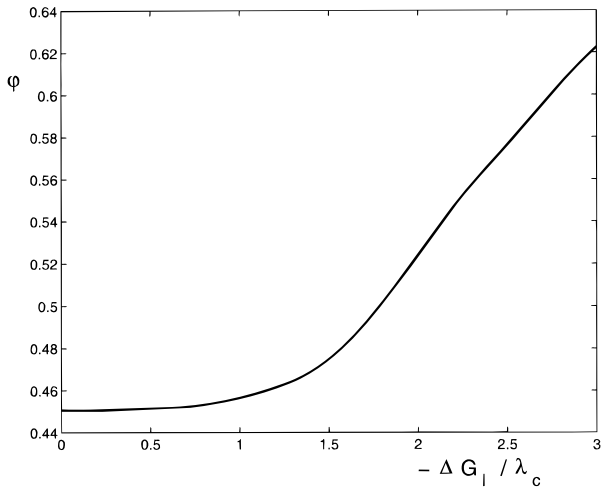

Figure 6. Averaged separation quantum yield $\bar{\varphi}$ as a function of ionization free energy $|\Delta G_i|$ at $w_r = w_i = 1.3 \times 10^3$ ns^{-1} and $r_c = 7$ Å (the other parameters are the same as in Figure 5).

4. Conclusions

The diffusion coefficient $\tilde{D}$ in eq 1.5 accounts for only diffusional separation of an ion pair while diffusional dependence $Z(\tilde{D})$ is of a different origin. The latter accounts for diffusional attainment of the recombination layer by ions created either inside or outside it. The exponential model takes into account only the first factor because the second is absent if ions are assumed to appear just at the place where they recombine. If this is not the case, the model remains qualitatively valid only in the fast diffusion (weak recombination) limit when the initial distribution of ions is spread so soon that its starting shape and position are practically insignificant. This is what we call *kinetic limit* of geminate recombination when $Z \approx z = \text{const}$. Oppositely, in the *diffusion-controlled* limit $Z(\tilde{D})$ dependence is essential and qualitatively different for inner and outer creation of charges. This criterion may be used to discriminate between kinetic and diffusional regimes and to identify the constitution of donor−acceptor energy space (NI, IN, II, or NN cases).

The same aim may be attained by study the free energy dependence of separation quantum yield. By changing the recombination free energy at fixed excitation quantum ϵ, one may obtain the complex distortion of the free energy gap law near the activationless region[3,4] which is indicative of diffusion control and qualitatively different in NI and IN cases. Alternatively, one may keep the recombination free energy fixed, changing only ionization free energy. The idea conceived here may serve as an *experimentum crucis* for the validity of the exponential model which denies any dependence of quantum yield on ionization free energy. In actual fact, this dependence is very weak until ions are generated deep inside the recombination layer but becomes very pronounced in the opposite case. So, it may also help to make a choice between inner and outer ionization with respect to the remote recombination layer.

Acknowledgment. The authors are grateful to Dr. P. Frantsuzov and A. Sivachenko for the help in preparing some figures.

References and Notes

(1) (a) Gould, I. R.; Moser, J. E.; Armitage, B.; Farid, S.; Goodman, J. L.; Herman, M. S. *J. Am. Chem. Soc.* **1989**, *111*, 1917. (b) Grampp, G.; Hetz, G. *Ber. Bunsen-Ges. Phys. Chem.* **1992**, *96*, 198. (c) Bolton, J. R.; Archer, M. D. In *Electron Transfer in Inorganic, Organic and Biological Systems*; Bolton, J. R., Mataga, N., McLendon, G., Eds.; Advances in Chemistry Series 228; American Chemical Society: Washington, DC, 1991; Chapter 2.

(2) (a) Burshtein, A. I. *Chem. Phys. Lett.* **1992**, *194*, 247. (b) Burshtein, A. I.; Krissinel, E.; Mikhelashvili, M. S. *J. Phys. Chem.* **1994**, *98*, 7319.

(3) Burshtein, A. I.; Krissinel, E. *J. Phys. Chem.* **1996**, *100*, 3005.

(4) Burshtein, A. I. *J. Chem. Phys.* **1995**, *103*, 7927.

(5) (a) Brunschwig, B. S.; Ehrenson, S.; Sutin, N. *J. Am. Chem. Soc.* **1984**, *106*, 6859. (b) Burshtein, A. I.; Morozov, V. A. *Chem. Phys. Lett.* **1990**, *165*, 432.

(6) Burshtein, A. I.; Frantsuzov, P. A.; Zharikov, A. A. *Chem. Phys.* **1991**, *155*, 91.

(7) (a) Monchick L. *J. Chem. Phys.* **1956**, *24*, 381. (b) Hong, K. M.; Noolandi, J. *J. Chem. Phys.* **1978**, *68*, 5163.

(8) Burshtein, A. I.; Zharikov, A. A.; Shokhirev, N. V.; Spirina, O. B.; Krissinel, E. B. *J. Chem. Phys.* **1991**, *95*, 8013.

(9) Burshtein, A. I.; Kofman, A. G. *Opt. Spectrosc.* **1976**, *40*, 175.

(10) Frantsuzov, P. A.; Shokhirev, N. V.; Zharikov, A. A. *Chem. Phys.* **1995**, *236*, 30.

(11) Yoshimori, A.; Watanabe, K.; Kakitani, T. *Chem. Phys.* **1995**, *201*, 35.

(12) Burshtein, A. I.; Frantsuzov, P. A. *Chem. Phys. Lett.*, in press.

(13) Matsuda, N.; Kakitani, T.; Denda, T.; Mataga, N. *Chem. Phys.* **1995**, *190*, 83.

(14) Burshtein, A. I.; Kofman, A. G. *Opt. Spectrosc.* **1976**, *40*, 175.

(15) Frantsuzov, P. A.; Shokhirev, N. V.; Zharikov, A. A. *Chem. Phys. Lett.* **1995**, *236*, 30.

(16) Tachiya, M. *J. Chem. Phys.* **1979**, *71*, 1276.

(17) Marcus. *J. Chem. Phys.* **1956**, *24*, 966; *Ibid* **1965**, *43*, 679.

(18) Burshtein, A. I.; Zharikov, A. A.; Shokhirev, N. V. *J. Chem. Phys.* **1992**, *96*, 1951.